Materials Today Communications 44 (2025) 112092

Contents lists available at ScienceDirect

Materials Today Communications

journal homepage: www.elsevier.com/locate/mtcomm

Cross-linked polyrotaxane based aerogel as supporter for leakage-proof phase change materials with high enthalpies

Hui Shi [a,b], Xiao-Mei Yang [c,d,*,1], Jun Mo [a], Huan Wang [a], Deming Tan [a], Guang-Zhong Yin [c,**,2]

[a] School of Mechanical Engineering, Chengdu University, Chengdu 610106, China
[b] Department of Chemical Engineering, Imperial College London, South Kensington Campus, London SW7 2AZ, UK
[c] Advanced Sustainable Polymers Lab, Escuela Politécnica Superior, Universidad Francisco de Vitoria, Ctra. Pozuelo-Majadahonda Km 1.800, Pozuelo de Alarcón, Madrid 28223, Spain
[d] Faculty of Diseño, Innovación y Tecnología, Universidad de Diseño, Innovación y Tecnología (UDIT), Av. Alfonso XIII, 97, 28016 Madrid, Spain

ARTICLE INFO

Keywords:
Polyrotaxane
Phase change materials
Heat treatment
Energy materials
PEG

ABSTRACT

We developed a series of cross-linked polyrotaxane (C-PLR)-based aerogels using hexamethylene diisocyanate (HDI) as a crosslinker. These aerogels were subsequently used as support materials for the encapsulation of poly (ethylene glycol) (PEG), resulting in stable and leakage-proof PCM composites with high enthalpies. The pore morphology was characterized using scanning electron microscopy (SEM). The excellent compatibility between the aerogels and PEG resulted in PCMs with outstanding anti-leakage properties. We characterized the phase change behavior of the material using a DSC, including phase change latent heat, supercooling, heat loss, and cycling stability. It is particularly noteworthy that these PCMs exhibited impressive cycle stability and an ultra-high latent heat of 182.34 J g^{-1} . We further designed a simple thermal management model to illustrate the heat regulation function of the PCM. The results showed that maintained much lower temperatures than those without PCM protection. In summary, this work introduces a novel aerogel-encapsulated PEG technique using crosslinked PLR aerogels. This encapsulation allows for a homogeneous integration of the support material and PCM work substance in molten and solid states. It presents a new and effective strategy for shape-stabilized, PEG-based PCMs to prevent leakage during phase transition.

1. Introduction

Phase change materials (PCMs) have garnered significant attention in recent years due to their potential in thermal energy storage applications [1–3]. These materials can absorb and release large amounts of latent heat during phase transitions, making them crucial for enhancing energy efficiency in various sectors, including building temperature regulation [4,5], electronic device cooling [6–8], and renewable energy systems [1,9,10]. Among the various PCMs, poly (ethylene glycol) (PEG) stands out due to its favorable thermal properties, non-toxicity, and chemical stability [11–14]. However, one of the primary challenges associated with PEG and other PCMs is leakage during phase transitions, which limits their practical application and performance.

To address these issues, researchers have explored various support materials and encapsulation techniques to enhance the shape stability and anti-leakage properties of PCM [15,16]. Our previous reports demonstrated that polyrotaxane (PLR) is an ideal support material for PEG in creating leakage-proof PCMs, due to its main chain chemical structure being identical to that of the PEG work substance [17–19]. The advanced PCMs for encapsulating PEG, fabricated using PLR as supports, can be easily extruded and remolded, providing a technical premise and convenience for large-scale applications. These composites have high phase change enthalpies (116.1–162.2 J/g) and very high enthalpy efficiency (>100 %) [18].

* Correspondence to: Faculty of Design, Innovation and Technology, University of Design, Innovation and Technology (UDIT), Av. Alfonso XIII, 97, Madrid 28016, Spain.
** Corresponding author.
E-mail addresses: xiaomei.yang@udit.es (X.-M. Yang), amos.guangzhong@ufv.es (G.-Z. Yin).
[1] ORCID: 0000-0002-3703-6651
[2] ORCID: 0000-0003-0065-2706

https://doi.org/10.1016/j.mtcomm.2025.112092
Received 24 October 2024; Received in revised form 4 January 2025; Accepted 2 March 2025
Available online 3 March 2025

The development of high enthalpy is a very important focus for phase change materials. Although the PLR system is an ideal carrier, there is still much room for improvement in phase change enthalpy. Aerogel encapsulation is a highly efficient method for preparing high enthalpy PCMs [20–22]. PLR aerogels, with their chemical structure, low density, and high porosity, emerge as promising candidates. However, initial attempts revealed that pure PLR foams tend to collapse during PEG absorption, making it difficult for the PCM to retain its shape. This issue likely arises from high porosity, imperfect cyclodextrin crystallization, and thermoplastic nature of PLR [23,24].

In this study, we anticipate that PLR aerogel alone will exhibit excellent absorption potential, while the PEO chains within PLR will ensure optimal compatibility between the foam and the PCM working substance. Utilizing hexamethylene diisocyanate (HDI) as a cross-linking agent, we will employe a one-step chemical cross-linking method to develop a series of cross-linked network PLR aerogels, without the need for additional support materials. Our objective is to create a novel PCMs support material with high encapsulation ratio, high enthalpy value as well as the enthalpy efficiency, robust shape stability, and anti-leakage properties, capable of effectively encapsulating PEG and preventing leakage.

2. Experimental section

2.1. Materials and methods

Poly (ethylene oxide) (PEO) with a weight-average molar mass of 1×10^6 g mol^{-1} and α-cyclodextrin (α-CD, 98 %) were purchased from Meryer and used as received. Polyethylene glycol (PEG) with a weight-average molar mass of 6000 g mol^{-1} was obtained from West Asia Chemical Technology (Shandong) Co., Ltd. 1,6-diisocyanatohexane (HDI, ≥99.0 % (GC)), Stannous octoate (92.5–100.0 %), n-Hexane (≥99 % (GC), ACS reagent), and dichloromethane (DCM, suitable for HPLC, ≥99.8 %) were purchased from Sigma Aldrich and used without any treatment. Deionized water was made in the laboratory.

2.2. Preparation of C-PLR

PEO (5 g) was dissolved in 150 mL of H_2O at 80 °C overnight. α-CD was then slowly added at mass ratios of 10 %, 20 %, and 30 %, to prepare sample 10 %PLR, 20 %PLR and 30 %PLR, respectively. After stirring overnight at room temperature, the reaction mixture was cooled down and stored in the refrigerator at 4 °C for 72 h to yield the corresponding inclusion complex solutions. The solutions were then transferred to several containers and freeze-dried. The resulting porous materials were placed in a solvent mixture (v/v=10/1) of n-hexane and hexamethylene diisocyanate, with stannous octoate (0.5 wt%) as the catalyst. After 48 h, the HDI-crosslinked C-PCR was taken out and washed with n-hexane. The wet aerogels were then dried in the vacuum oven at temperature of 55 °C for 24 h, to generate sample C-10 %PLR, C-20 %PLR, and C-30 % PLR (See Table 1 for the key parameters for the aerogels).

2.3. Preparation of C-PCMs

Finally, molten PEG was adsorbed into crosslinked PLR aerogels at 80 °C in a vacuum oven. The pristine PLR aerogels (without crosslinking treatment) were also used to absorb PEG to prepare the PCMs and served as the references (see Table 2 for more details).

Table 1
Porosity and gel contents of crosslinked PLR aerogels.

Samples	Bulk density ρ (g/cm^3)	$\rho_{aerogel}$ (g/cm^3)	Porosity (%)	Gel content %
C−10 % PLR	1.41	0.128±0.002	90.9	97.2±0.2
C−20 % PLR	1.41	0.131±0.004	90.7	98.1±0.1
C−30 % PLR	1.42	0.144±0.001	90.6	98.9±0.1

2.4. Characterizations

(1) Gel content. We used excess DCM to soak the resulting cross-linked PLR aerogels and then calculate the gel content of the aerogels according to the following formula (1):

$$Gel\ content\% = \frac{m}{m_0} \times 100 \quad \% \tag{1}$$

where m is the initial mass, and m_0 is the mass after DCM immersion.

(2) Porosity. The porosity of the C-PLR aerogels can be calculated using formula (2) [25]:

$$\text{Porosity}\% = \frac{\rho - \rho_{aerogel}}{\rho} \times 100 \quad \% \tag{2}$$

where ρ represent the bulk density of aerogel and $\rho_{aerogel}$ is the density of aerogel.

(3) PEG loading. The loading capacity was used to determine the PEG content adsorbed in C-PCMs. Typically, the C-PCMs were weighed before (m_1) and after (m_2) PEG adsorption. At least three samples of each film were analyzed. The loading capacity was calculated using the following equation:

$$loading\% = \frac{m_2 - m_1}{m_2} \times 100 \quad \% \tag{3}$$

(4) Morphology. Scanning electron microscope (SEM, Hitachi S-4800) was used to observe the surface morphology of PCMs and cross section morphology after adsorption of PEG. The samples were heated at 80 °C for 3 h to detect the leakage and shape change. The weight loss after heat treatment were calculated using the following equation:

$$loading\% = \frac{m_0 - m_t}{m_0} \times 100 \quad \% \tag{4}$$

where, m_0 is the initial weight of form stable PCM and m_t is the weight of the PCM after heat treatment.

(5) Phase change performance and cycle stability. Differential scanning calorimetry (DSC) analysis was performed for each film (5–10 mg) using a TA-Q200 in a N_2 atmosphere (50 mL min^{-1}). Generally, the samples were heated from 30 °C to 100 °C at a speed of 10.00 °C min^{-1}; then cooled to 30 °C at the same speed; lastly heated to 100.00 °C at 10.00 °C min^{-1}. **Cycle-stability test**. The sample C-PCM-10 % was selected for 45 cycles. Both heating and cooling procedures were used to test at 10 °C min^{-1} from 30 ºC to 100 ºC. To calculate the change of exothermic and endothermic heat as well as the enthalpy efficiency and phase change temperatures.

(6) Thermal conductivity. Thermal conductivity measurements were performed using a thermal constants analyzer (TPS2500 S, Hot Disk) at room temperature. Reported results demonstrate the average of three measurements for each sample (with thickness of ~4 mm) to ensure repeatability.

3. Results and discussion

3.1. Preparation of the C-PLR aerogel and PEG encapsulation

In previous reports, we know that polyrotaxane itself is also a phase change material with good comprehensive properties. [17] To achieve a higher phase change heat storage capacity, we utilize PLR to prepare aerogels, specifically the reference samples PLR-10% and PLR-30% in this study. These aerogels are designed to serve as support materials for loading additional PEG working substances. However, their inherent thermoplasticity and high porosity lead to challenges in maintaining

Table 2
DSC results for key parameters of Phase change materials.

Samples	$T_{m,\ onset}$ (°C)	$T_{s,\ onset}$ (°C)	Melting Enthalpy (J/g)	Solidification enthalpies (J/g)	Loading (%)	Enthalpy efficiency (%)	Extent of supercooling (°C)	Heat loses (%)	Thermal conductivity (W/(m•K))
C-PCM−10 %	57.86	45.80	182.34	176.94	93.79	110.33	12.06	2.96	0.2292
C-PCM−20 %	57.38	46.19	164.33	160.68	90.86	102.65	11.19	2.22	0.2877
C-PCM−30 %	57.22	46.00	156.12	150.11	90.94	97.43	11.22	3.84	0.3306

Note: the extent of supercooling and heat lose were both calculated according to the first cycle in DSC results.

structural integrity, resulting in significant collapse when they absorb PEG6K in its molten form. Consequently, this study focuses on employing a classic polyurethane cross-linking method using HDI to reinforce the aerogel, with the goal of creating more stable three-dimensional support frameworks. Fig. 1(a) illustrates the preparation process of HDI-crosslinked PLR (C-PLR). In this process, HDI reacts with the hydroxyl groups on PLR to form urethane bonds, creating a cross-linked three-dimensional network that enhances the self-standing capacity during PEG absorption. PLR consists of cyclic α-CDs, threaded onto a linear polymer chain, which often contains hydroxyl groups. The cross-linking process includes the following steps: (1) Isocyanate-Hydroxyl Reaction: reactive isocyanate groups (-NCO) of HDI react with the hydroxyl groups (-OH) on the cyclic molecules or the linear polymer chain of the PLR, forming urethane linkages (-NH-CO-O-); (2) Formation of cross-links: Each HDI molecule can react with two hydroxyl groups, either on the same or different PLR molecules, resulting in a network of urethane bonds that cross-link the PLR chains.

The density, porosity and gel content results of the C-PLR aerogels after cross-linking are presented in Table 1. We found that all the C-10 % PLR, C-20 % PLR, and C-30 % PLR samples have similar porosity, reaching up to 90 %. This is primarily due to the fact that the porosity is largely determined by the concentration of the polymer used in preparation. Using Eq. (1), we calculated the gel content of the cross-linked aerogels. Specifically, we observed that the overall gel content is very high, exceeding 97 %. Furthermore, we noted a relatively smooth increasing trend in gel content among the C-10 % PLR, C-20 % PLR, and C-30 % PLR samples. This can be attributed to the probabilistic increase in the number of cross-linking points formed by cyclodextrins. Consequently, samples with higher cyclodextrin content demonstrate a more complete cross-linking network.

The crosslinked aerogels were obtained and then impregnated with molten PEG under vacuum conditions to achieve PEG loading. For comparison, we also prepared non-crosslinked PLR-10 %, PLR-20 %, and PLR-30 % samples loaded with PEG using the same method. The physical appearance of these samples is shown in Fig. 2(a). The non-crosslinked aerogels underwent significant shape collapse during the PEG absorption process. However, after crosslinking modification, the samples retained their original size and shape even after PEG absorption, as shown in Fig. 2(b). This clearly demonstrates that the crosslinking modification significantly improves the size stability of PLR aerogels when encapsulating PEG. Furthermore, based on Eq. (3), we can calculate the loading capacity of C-PLR-PCM samples, and the corresponding results are listed in Table 2. As can be seen, all the loading can exceed 90 %.

Fig. 3(a) illustrates the process of preparing C-PCMs by adsorbing and encapsulating PEG6K into C-PLR aerogel using vacuum-assisted impregnation. SEM observations (Fig. 3(b, c, d, b′, c′, and d′)) reveal a well-developed network and robust skeleton structure formed by the reaction between diisocyanate and hydroxyl groups. Changes in cyclodextrin concentrations do not notably affect the aerogel morphology. Regarding post adsorption and encapsulation of PEG, SEM images show a uniform morphology with PEG filling the porous network structure, indicating effective integration between the skeleton structure and PEG without visible phase separation. Notably, some cracks are visible in Fig. 3(d)'. This may be due to the limited amount of small PEG molecules filling the spaces between the microstructural units of the crosslinked aerogel. Upon cooling and crystallization, the crystallized PEG has a higher density compared to its molten state. As a result, after solidification, some space is released, leading to the formation of cracks.

3.2. C-PCMs performance

3.2.1. Shape stability and anti-leakage performance

The photos of C-PCM with varying concentrations of α-CD before and after heat treatment are shown in Fig. 4. After absorbing PEG6K, the

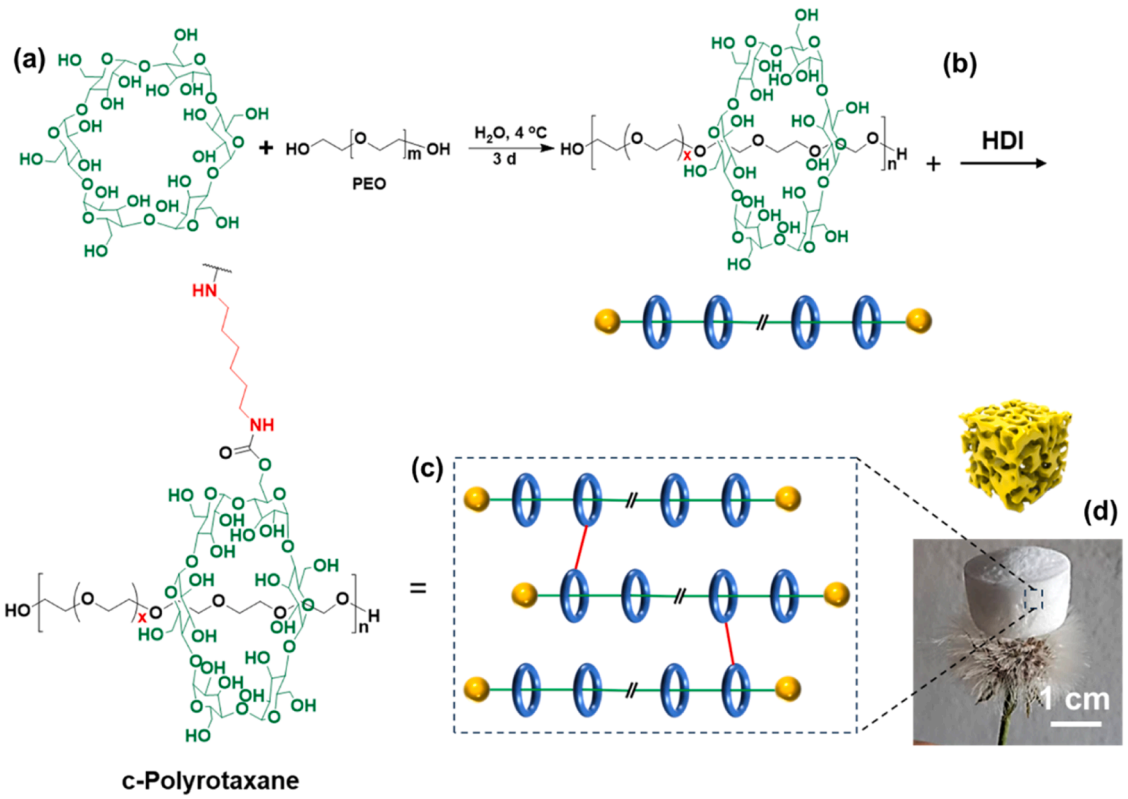

Fig. 1. C-PLR aerogel synthesis route: (a) Synthesis of Polyrotaxane, (b) Crosslinking of the PLR aerogel, (c) the illustration of the crosslinked PLR molecular structure, and (d) Image of typical PLR aerogel.

cross-linked PCMs maintained their morphology well even after being heated at 80 °C for 3 h. There was almost no deformation, demonstrating their strong form stability. Furthermore, the weight loss after heat treatment is 1.2±0.1 %, 1.3±0.1 % and 1.6±0.2 %, which directly reflects the material's excellent leakage resistance.

As illustrated in Fig. 5(a) and presented in our previous work [17, 18], in the molten state of the phase change material, both the support material and the PCM working substance undergo melting. In the solidified state, the main chain of PEO and the PEG working substance may form a eutectic, as shown in Fig. 5(b). Notably, Fig. 5(c) demonstrates that the main chain of the PLR support consists of a long PEO chain, which shares the same chemical structure as the short PEG6K chain. Unlike traditional inorganic aerogels or polysaccharide aerogels, the support material forms a homogeneous phase with the PEG working substances upon melting. This significantly reduces the risk of PEG leakage.

3.2.2. Phase change performance, cycle stability and thermal conductivity

Melting enthalpy can directly reflect the energy storage capacity of PCMs. Fig. 6(a) and (b) present the melting and solidification enthalpies, respectively, based on the heating and cooling curves of DSC data. The corresponding parameters are provided in Table 2. The melting enthalpies for sample C-PCM-10 %, C-PCM-20 % and C-PCM-30 % are 182.34 J/g, 164.33 J/g and 156.12 J/g, respectively. We found here that the melting enthalpy decreased with the increase of α-CD contents (gel content), which is mainly because a higher concentration of α-CD and the higher gel content restrains the mobility of the PLR chain to a certain extent, giving rise to relative low crystallinity accordingly. Furthermore, some parameters can be calculated for deeply understanding the PCMs, the enthalpy efficiency of PCMs can be determined by Eq. (5), [26]

$$\text{Enthalpy effic iency\%} = \frac{\Delta H_m}{\omega \Delta H_{PEG}} \times 100\% \quad (5)$$

where ΔHm (J/g) is the melting enthalpy of the C-PCMs with varying concentrations of α-CD, ΔH_{PCM} (J/g) represents the melting enthalpy of PEG, which is 176.2 J/g as tested in our previous work, [18] and ω (%) represents the loading of PEG in the C-PCMs with varying concentrations of α-CD. The calculated data can be found in Table 2. We observed that both C-PCM-10 % and C-PCM-20 % exhibit an enthalpy efficiency greater than 100 %. This is because the supporting material itself contributes to the phase change latent heat to a certain extent. However, when the cyclodextrin content reaches 30 % and the gel content is higher, the mobility of PEO in the aerogel decreases, reducing its contribution to the phase change enthalpy. As a result, the enthalpy efficiency is less than 100 %.

The extent of supercooling (ΔT, °C) was evaluated by the following equation:

$$\Delta T = T_{m,\ onset} - T_{s,\ onset} \quad (6)$$

where $T_{m,\ onset}$ represents the melting enthalpy, and $T_{s,\ onset}$ represents the solidification enthalpy. According to Eq. (6), the extent of supercooling for C-PCM-10 %, C-PCM-20 %, and C-PCM-30 % is calculated to be 12.06 °C, 11.19 °C, and 11.22 °C, respectively (Table 2), indicating that it remains almost unchanged relative to the reference samples, which are similar as other PLR materials systems.

The percentage of heat lose (η, %) was evaluated by Eq. (6):

$$\eta = (\Delta H\, m - \Delta H\, s)/\Delta H\, m \times 100\% \quad (7)$$

where, $\Delta H\, m$ (J/g) presents the melting enthalpy of the PCMs, and $\Delta H\, s$ (J/g) presents the solidification enthalpy. The results are all listed in Table 2.

The C-PCM-10 % sample showed a lower percentage of heat loss between endothermic and exothermic cycles compared to the other two samples, suggesting that the smaller amount of HDI crosslinker did not cause heat loss in the PEG within the PCMs. The PCMs maintained

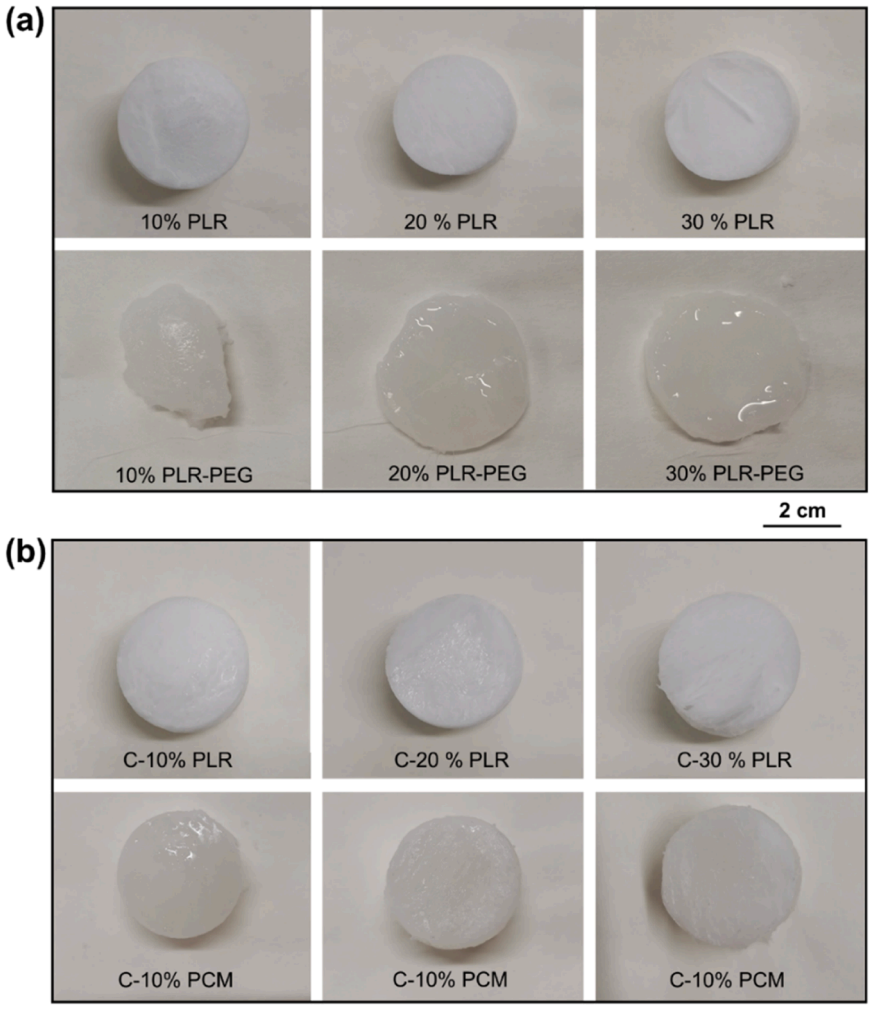

Fig. 2. Images of (a) PLR aerogels and PCMs; (b) C-PLR aerogels and C-PCMs.

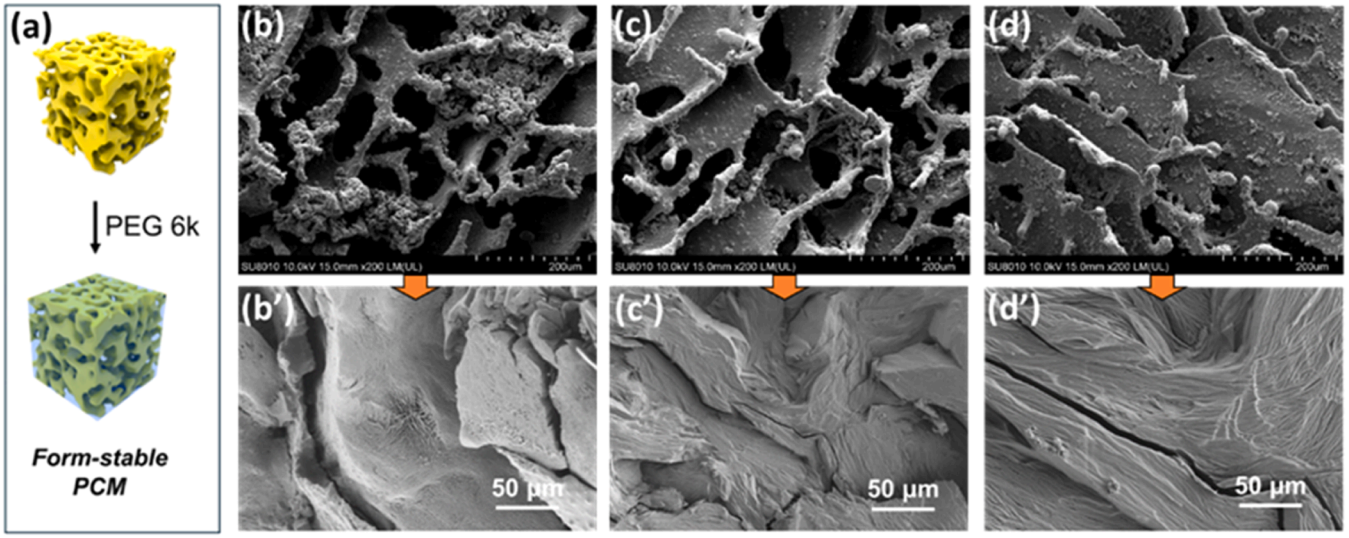

Fig. 3. (a) process of preparing C-PCMs by adsorbing and encapsulating PEG6K onto C-PLR aerogel with varying concentrations of α-CD; (b, c, d) morphology C-PLR aerogel with varying concentrations of α-CD; (b′, c′, d′) C-PCMs with varying contents of α-CD.

distinct melting and crystallization temperatures during the heating and cooling processes, indicating strong cycle performance. This is supported by the stability of key parameters—melting enthalpy, solidification enthalpy, and melting temperature—which remained consistent after 45 cycles (Fig. 5c, d, and e). Consequently, the C-PCM are regarded as high-performance, form-stable phase change materials

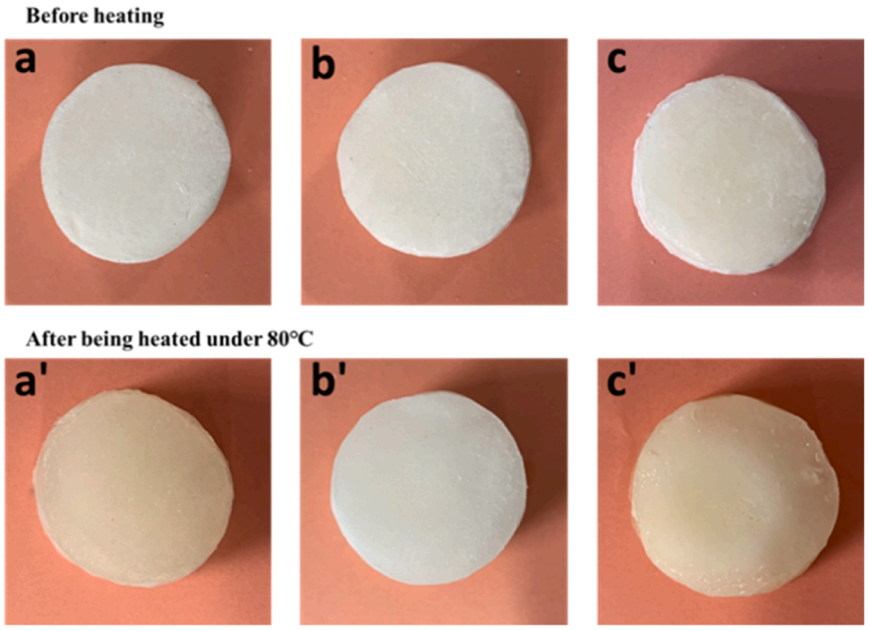

Fig. 4. Form stability of the samples: C-PCM-10 % (a), C-PCM-20 % (b), C-PCM-30 % (c) before heating, and C-PCM-10 % (a'), C-PCM-20 % (b') and C-PCM-30 % (c') after heating under 80 °C 3 h.

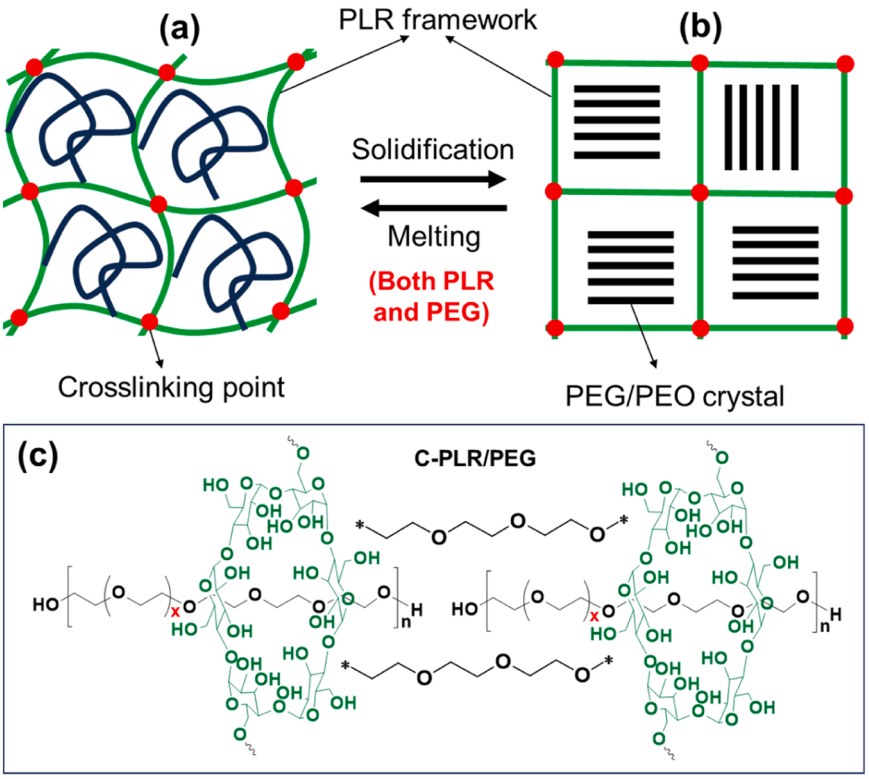

Fig. 5. (a) A microscopic diagram of the PCM composite in its molten state; (b) A microscopic diagram of the PCM composite at room temperature; (c) A schematic representation of the chemical structure of the PCM composite.

suitable for thermal energy storage. Notably, in Fig. 5(e), Cycle 1 has a distinct thermal history, which is why the first heating curve differs significantly from the subsequent cycles. However, after 45 cycles, we observed that the remaining cycles overlap almost perfectly, demonstrating the material's excellent cycle stability.

We also measured the thermal conductivity of the samples without any additional functional fillers. The results are listed in Table 2. Overall, the thermal conductivity is relatively low, ranging from 0.2292 to 0.3306 W/(m•K). We observed a slight increase in thermal conductivity as the cyclodextrin content increased. This may be due to the higher density of the supporting material after crosslinking, which slightly enhances heat conduction.[17]

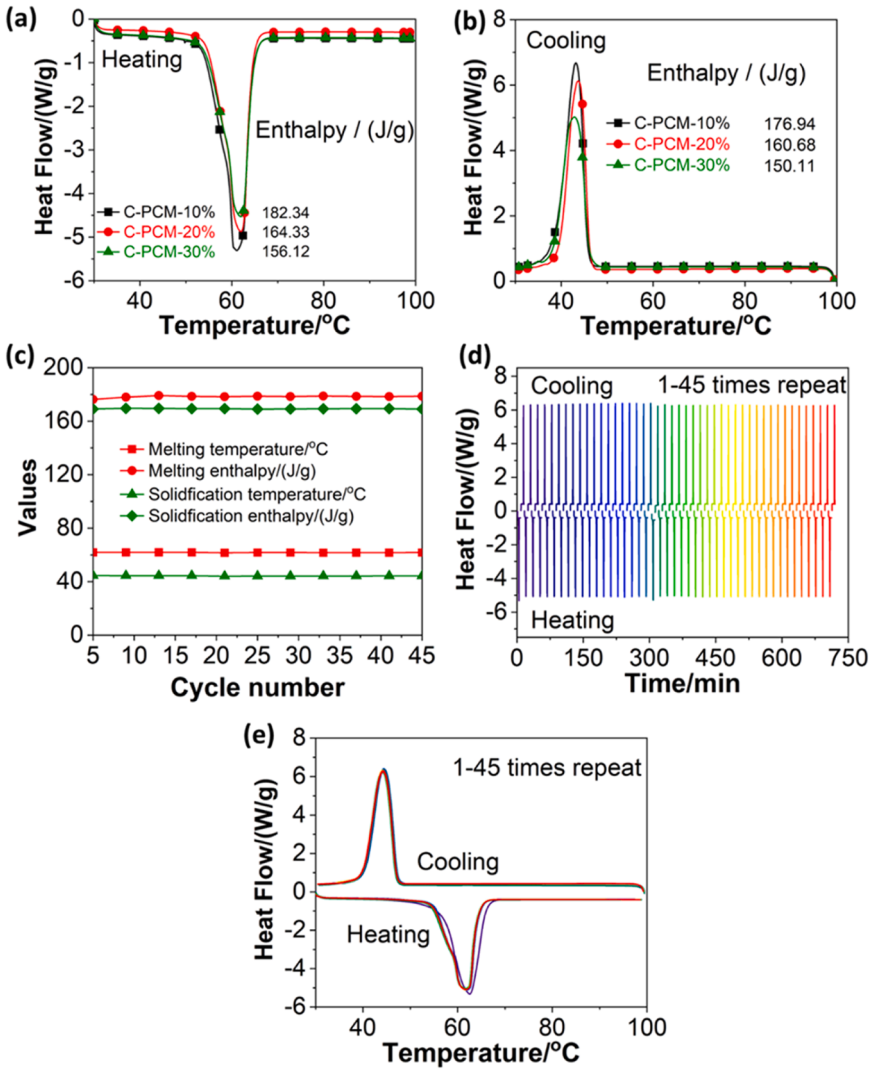

Fig. 6. (a) melting and (b) solidification enthalpies of C-PCMs with different α-CD contents at heating rate of 10 °C min $^{-1}$; (c) DSC cycle curves of C-PCMs (sample C-PCM-10 %); and (d and e) the cycle performance (including the parameters of enthalpy efficiency, latent heat, melting temperature and solidification temperature) of C-PCM- 10 % as a typical example.

3.2.3. Thermal management performance

Fig. 7(a) depicts the simulated device setup, featuring an insulation layer, protective sheet, and PCM arranged from bottom to top. Fig. 7(b) provides both a schematic and a top-view photograph of two PCM-equipped devices, illustrating the overall material testing system. In Fig. 7(c), IR images reveal the behavior of various samples under different heating durations. After 180 s of heating, the sample without C-PCM begins to heat up remarkably, while the sample with C-PCM shows no significant temperature change. The corresponding heating curves in Fig. 7(d) further confirm that, as heating time increases, the sample with C-PCM demonstrates markedly better temperature control compared to both the unprotected sample and a reference sample.[23] Notably, the protective sheet containing C-PCM maintains a temperature approximately 12 °C lower than the one without C-PCM. The results highlight the critical role of phase change enthalpy in managing thermal loads in electronic devices. The substantial and sustained temperature difference underscores the effectiveness of PCM in electronic thermal regulation.

4. Conclusion

HDI cross-linked PLR-encapsulated PEG6K composites with varying concentrations of α-CD (10 %–30 %) were successfully prepared. The introduction of the cross-linking agent HDI effectively prevented the collapse typically associated with pure PLR adsorption of PCM. This method is simple and efficient. After PCM adsorption, the melting enthalpy reached 182.34 J/g, while the solidification enthalpy reached 176.94 J/g when the CD content of PLR was 10 %. The PCM maintained stable melting enthalpy, solidification enthalpy, and melting temperature. Additionally, the protective sheet containing C-PCM maintained a temperature approximately 12 °C lower than the one without C-PCM. These results indicate that C-PCM is a high-performance, form-stable phase change material suitable for thermal energy storage. Notably, this work not only advances the design of leakage-proof and shape-stable PEG-based PCMs but also contributes to the broader field of sustainable energy storage solutions.

CRediT authorship contribution statement

Shi Hui: Writing – review & editing, Writing – original draft, Resources, Methodology, Data curation, Conceptualization. **Yang Xiao-Mei:** Writing – review & editing, Writing – original draft, Methodology, Investigation, Formal analysis, Data curation, Conceptualization. **Mo Jun:** Writing – review & editing, Formal analysis, Data curation. **Wang**

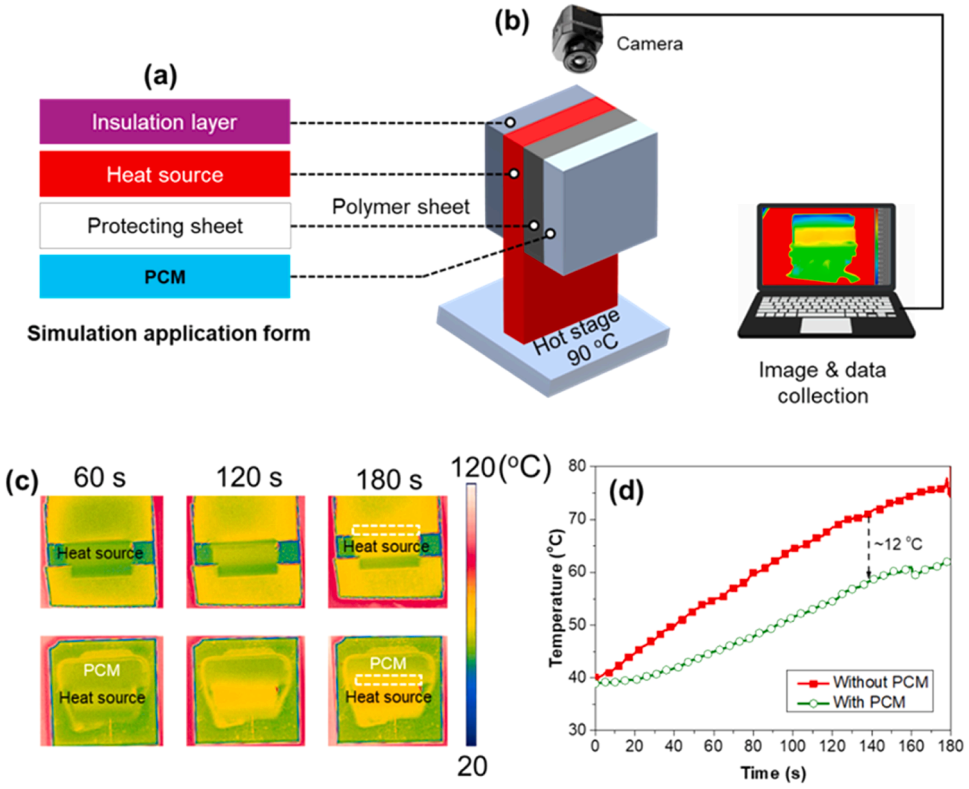

Fig. 7. (a) The layered structure of the simulated device; (b) test setup and device images; (c) IR images of representative samples, comparing the device with and without C-PCM; (d) heating curves for the protective sheet, comparing with and without C-PCMs.

Huan: Writing – review & editing, Formal analysis, Data curation. **Tan Deming:** Writing – review & editing, Formal analysis, Data curation. **Yin Guang-Zhong:** Writing – review & editing, Supervision, Resources, Project administration, Methodology, Investigation, Funding acquisition, Formal analysis, Data curation, Conceptualization.

Declaration of Competing Interest

The authors declare that they have no known competing financial interests or personal relationships that could have appeared to influence the work reported in this paper.

Acknowledgments

This work was supported by NEWSAFE (No.: PID2022-143324NA-I00) Projects funded by: MICIU (Ministerio de Ciencia, Innovación y Universidades)/AEI (Agencia Estatal de Investigación)/10.13039/501100011033 and, as appropriate, by "ERDF/EU"; and Ramón y Cajal Fellowship (No.: RYC2023-045023-I) funded by: MICIU, and, as appropriate, "ESF Investing in your future". This work was also partially supported by INC-UDIT-2025-PRO21 and China scholarship council.

Data availability

No data was used for the research described in the article.

References

[1] M. Samykano, Role of phase change materials in thermal energy storage: potential, recent progress and technical challenges, Sustain. Energy Technol. Assess. 52 (2022) 102234.
[2] W.P. Wong, A. Kagalkar, R. Patel, P. Patel, S. Dharaskar, R. Walvekar, M. Khalid, V. V. Gedam, Nano-enhanced phase change materials for thermal energy storage: a comprehensive review of recent advancements, applications, and future challenges, J. Energy Storage 74 (2023) 109265.
[3] L. Yang, X. Jin, Y. Zhang, K. Du, Recent development on heat transfer and various applications of phase-change materials, J. Clean. Prod. 287 (2021) 124432.
[4] X. Wang, W. Li, Z. Luo, K. Wang, S.P. Shah, A critical review on phase change materials (PCM) for sustainable and energy efficient building: design, characteristic, performance and application, Energy Build. 260 (2022) 111923.
[5] K. Faraj, M. Khaled, J. Faraj, F. Hachem, C. Castelain, A review on phase change materials for thermal energy storage in buildings: heating and hybrid applications, J. Energy Storage 33 (2021) 101913.
[6] Y. Liu, R. Zheng, J. Li, High latent heat phase change materials (PCMs) with low melting temperature for thermal management and storage of electronic devices and power batteries: critical review, Renew. Sustain. Energy Rev. 168 (2022) 112783.
[7] K. Du, J. Calautit, Z. Wang, Y. Wu, H. Liu, A review of the applications of phase change materials in cooling, heating and power generation in different temperature ranges, Appl. Energy 220 (2018) 242–273.
[8] H. Hu, Recent advances of polymeric phase change composites for flexible electronics and thermal energy storage system, Compos. Part B Eng. 195 (2020) 108094.
[9] A. Safari, R. Saidur, F.A. Sulaiman, Y. Xu, J. Dong, A review on supercooling of phase change materials in thermal energy storage systems, Renew. Sustain. Energy Rev. 70 (2017) 905–919.
[10] S.F. Ahmed, N. Rafa, T. Mehnaz, B. Ahmed, N. Islam, M. Mofijur, A.T. Hoang, G. M. Shafiullah, Integration of phase change materials in improving the performance of heating, cooling, and clean energy storage systems: an overview, J. Clean. Prod. 364 (2022) 132639.
[11] T.L. Wong, K.Abeykoon C. Ma, Enhancing the thermal performance of polyethylene glycol phase change material with carbon-based fillers, Int. J. Heat. Mass Transf. 220 (2024) 124919.
[12] H. Jiang, C. Yang, J. Song, P. Cao, J. Chen, J. Wang, W. Hong, Efficient enhancement of heat storage capacity of polyethylene glycol phase change material based on a novel fly ash support, ACS Sustain. Chem. Eng. 12 (19) (2024) 7382–7391.
[13] K. Yan, Y. Feng, L. Qiu, Thermal and photo/electro-thermal conversion characteristics of high energy storage density expanded graphite/polyethylene glycol shaped composite phase change materials, Sol. Energy 272 (2024) 112477.
[14] X. Guo, K. Wei, T. Ni, W. Shi, C. Dai, Z. Zhao, Z. Gu, Preparation and performance analysis of polyethylene glycol/epoxy resin composite phase change material, J. Energy Storage 88 (2024) 111525.
[15] K. Palraj, D. Shanmugavel, Development of form-stable natural composite phase change material for effective thermal energy storage and anti-leakage behaviour, J. Energy Storage 84 (2024) 110692.
[16] R. Chen, D. Li, N. Sheng, C. Zhu, Direct synthesis of porous aluminum nitride foams for enhancing heat transfer and anti-leakage performance of phase change materials, Thermochim. Acta 734 (2024) 179706.

[17] G.-Z. Yin, J. Hobson, Y. Duan, D.-Y. Wang, Polyrotaxane: new generation of sustainable, ultra-flexible, form-stable and smart phase change materials, Energy Storage Mater. 40 (2021) 347–357.
[18] G.-Z. Yin, A. Marta López, X.-M. Yang, X. Ao, J. Hobson, D.-Y. Wang, Polyrotaxane based leakage-proof and injectable phase change materials with high melting enthalpy and adjustable transition temperature, Chem. Eng. J. 444 (2022) 136421.
[19] F. Bétermier, N. Daher, L.A. Blanquer, J. Brun, A. Marcellan, N. Jarroux, J.-M. Tarascon, Understanding the electrochemical performances of Si anodes incorporating mechanically interlocked binders prepared from α-cyclodextrin-based polyrotaxanes, Chem. Mater. 35 (3) (2023) 937–947.
[20] X. Zuo, X. Zhang, Y. Tang, Y. Zhang, X. Li, H. Yang, Preparation of serpentine fiber/poly (vinyl alcohol) aerogel with high compressive strength to stabilize phase change materials for thermal energy storage, Appl. Clay Sci. 247 (2024) 107214.
[21] Q. Guo, H. Yi, F. Jia, S. Song, Novel MoS2/montmorillonite hybrid aerogel encapsulated PEG as composite phase change materials with superior solar-thermal energy harvesting and storage, J. Colloid Interface Sci. 667 (2024) 269–281.
[22] Z. Cheng, S. Li, X. Tong, P. Chen, M. Zeng, Q. Wang, Material preparation and heat transfer characterization of porous graphene aerogel composite phase change material, Int. Commun. Heat. Mass Transf. 152 (2024) 107280.
[23] G.-Z. Yin, A.M. López, I. Collado, A. Vázquez-López, X. Ao, J. Hobson, S. G. Prolongo, D.-Y. Wang, MXene multi-functionalization of polyrotaxane based PCMs and the applications in electronic devices thermal management, Nano Mater. Sci. 6 (5) (2024) 495–503.
[24] G.-Z. Yin, X.-M. Yang, A.M. López, J.G. Molleja, M.-T. Wang, D.-Y. Wang, Graphene functionalization of polyrotaxane-encapsulated PEG-based PCMs: fabrication and applications, Adv. Mater. Technol. 8 (19) (2023) 2300658.
[25] Lee Joohyoung, Han Hyesu, Noh Dowon, Lee Jeongwoo, Daniel Lim Dahyun, Park Jinwoo, X.Gu Grace, Choi Wonjoon, Multiscale porous architecture consisting of grapheneaerogels and metastructures enabling robust thermal and mechanical functionalities of phase change materials, Adv. Funct. Mater. 34 (2024) 2405625.
[26] P. Cheng, H. Gao, X. Chen, Y. Chen, M. Han, L. Xing, P. Liu, G. Wang, Flexible monolithic phase change material based on carbon nanotubes/chitosan/poly(vinyl alcohol), Chem. Eng. J. 397 (2020) 125330.